Quantum Electronics **51** (12) 1107–1112 (2021)

https://doi.org/10.1070/QEL17661

Reflectogram shape deformation in distributed fibre systems in the presence of spontaneous noise in the probe radiation

N.I. Kalmykov, D.A. Kovalenko, I.A. Lobach, S.I. Kablukov

Abstract. **We report a study of the effect of spontaneous emission-induced noise in probe pulsed radiation on the reflectogram shape deformation in a distributed temperature sensor based on Raman scattering of light. Since the fraction of spontaneous emission in the used erbium-doped amplifier can reach 50% of the total power, this leads to deviations of reflectograms in the temperature sensor from the theoretical exponential dependence and, as a result, can yield a temperature measurement error of several degrees. Filtering the radiation with an amplitude modulator makes it possible to reduce these deviations. The influence of spontaneous emission on reflectograms is studied theoretically and experimentally.**

Keywords: *distributed temperature sensor, Raman scattering of light, spontaneous emission, reflectogram, spectral filtering.*

1. Introduction

With the progress of technologies in industry, construction, oil and gas production, as well as in other areas, the structure complexity of buildings, installations, technical units and devices is increasing. As a result, diagnostics and monitoring of their technical condition become of particular importance. The most advanced trend in monitoring is the use of fibre-optic methods for measuring physical parameters. The advantages of fibre-optic sensors include their low weight and size, the absence of electrical signals in the measuring path, insensitivity to electromagnetic interference and the effects of aggressive media; therefore, such sensors can be used under conditions of increased explosiveness, strong electromagnetic and radio frequency exposures, as well as in contact with flammable mixtures. Distributed fibre sensor systems (DFSS's) occupy a special place among all fibre-optic sensors, which literally opened a new technological era in metrology and solved many practical problems. Such systems consist of a sensing element (ordinary optical fibre) and an interrogator, which generates a probe optical signal and analyses the scattered signal returned from the sensor. Since the local measurement of physical parameters using these sensors provides a unique opportunity to monitor long objects, distributed sensors are a promising alternative to multiplexed point sensors. One fibre-optic cable can potentially replace thousands of point sensors, greatly simplifying both the measurement setup itself and the process of interrogation of the sensors [1–3]. Currently, fibre-optic sensors are used to measure the distribution of temperature [4–10], deformations [11, 12] and vibroacoustic effects [13, 14] in various objects.

The principle of operation of distributed systems is based on the method of pulsed optical reflectometry [1], when a series of short probe pulses is launched into a fibre line and the intensity of scattered radiation with a time is recorded for each pulse. Then, using the 'echo' principle, the reflectogram, that is, the dependence of the scattered radiation parameters on time (the length of the fibre line) is measured. In an optical fibre, there are three main types of light scattering [1], namely, Rayleigh, Brillouin, and Raman scattering; exactly they are used in DFSS's. It is essential that the characteristics of the scattered radiation can be susceptible to the magnitude of a physical impact, which allows measuring its distribution along the fibre. DFSS's can also be classified based on scattered radiation characteristics; here a distinction is made between spectral and amplitude approaches. In particular, DFSS's based on Brillouin scattering of light [11] are mainly spectral, because they take advantage of the fact that the optical spectrum of the scattered radiation changes with the local temperature and/or deformation of the fibre. A number of DFSS's are amplitude sensors. Thus, in DFSS's based on Raman scattering (RS), the local temperature in the fibre is related to the intensity of the scattered radiation [4]. It should be noted that such sensors are actively used to monitor the temperature in oil and gas wells, and in fire safety systems [6], when working with explosive materials. The detection of bosonic components of the RS makes it possible to use such sensors for measuring ultralow temperatures [7]. Because of the small fraction of scattered radiation in the amplitude DFSS's, special attention is paid to the correctness of measuring the signal amplitude and reducing its noise component. In particular, highly sensitive photodetectors [8] and/or various filtering systems [9] are used. Note also that distributed signal amplification allows obtaining information from a line with a length close to 100 km [10].

The source of probe radiation (PR) in an interrogator plays an important role in DFSS's. Obviously, a low peak power of the PR pulses leads to a decrease in the signal-to-noise ratio and decreases the accuracy of the physical parameter measurement. Therefore, to reduce the noise, it is necessary to carry out a long-term accumulation of the signal, which makes the measuring system more inertial. The signal-to-noise ratio can be increased by using a higher output power of the PR. In this approach, due to the high cost of

N.I. Kalmykov, I.A. Lobach, S.I. Kablukov Institute of Automation and Electrometry, Siberian Branch, Russian Academy of Sciences, prosp. Akad. Koptyuga 1, 630090 Novosibirsk, Russia; e-mail: kalmykov@iae.nsk.su, lobach@iae.nsk.su, kab@iae.nsk.su;
D.A. Kovalenko SibSensor LLC, Inzhenernaya ul. 20, 630090 Novosibirsk, Russia; e-mail: kovalenko@i-sensor.ru

Received 15 September 2021
Kvantovaya Elektronika **51** (12) 1107–1112 (2021)
Translated by V.L. Derbov

high-power laser sources, as a rule, a scheme with a low-power pulsed master laser and an optical amplifier is used, the amplifier often being a fibre one. Thus, in Ref. [9], an erbium-doped fibre amplifier was used for such purposes. Unfortunately, in this case, the amplifier not only amplifies the pulse amplitude, but can also introduce additional noise into the probe radiation.

Here we investigate the effect of spontaneous radiation (SR) generated in an erbium-doped fibre amplifying path on the shape distortion of reflectograms. DFSS temperature measurement based on RS was chosen as the object of research. It is shown that SR experiences RS, which is detected by the receiving part of the system and, in turn, gives rise to a time-dependent addition to the recorded signal and to the reflectogram distortion. Analytical expressions for the scattering signal from SR are obtained and experimentally confirmed. A method for spectral filtering of probe radiation using an amplitude light modulator is proposed. It is shown that the proposed filtering method allows the quality of reflectograms to be improved and, consequently, the temperature measurement errors to be reduced in the DFSS.

2. Experiment

In this work, we studied the DFSS for measuring temperatures with a line length of up to 16 km (Fig. 1). The PR source of the device consisted of a pulsed diode laser with a wavelength near 1550 nm and an erbium-doped amplifier to increase the peak radiation power; the duration and repetition rate of the PR pulses were 10 ns and 6.3 kHz, respectively. The erbium-doped amplifier had a double-pass scheme with counterpropagating diode pumping, similar to that described in Refs [15, 16]. A fibre Bragg grating (FBG) was used to provide the second pass and spectral filtering of the pulses. The average output power at the amplifier output, including the SR power, reached 3 mW. Through a Raman wavelength division multiplexer (RWDM) playing the role of a spectrally selective filter, the amplified pulsed radiation was injected into a standard telecommunications multimode fibre (at a constant temperature) with a core diameter of 62.5 μm and a length of 16 km. The backscattered signal was detected using two photodetectors. The reflectograms of backscattered signals at Stokes (1630 nm) and anti-Stokes (1430 nm) wavelengths were analysed.

Analysis of the PR spectrum, measured with a Yokogawa AQ6370 spectrum analyser, showed, in addition to the main line near 1550 nm, the presence of a broadband plateau (Fig. 2a). This additional signal, caused by SR in the erbium-doped fibre amplifier because of using the double-pass amplification scheme, contains two components. A relatively narrow peak near 1550 nm corresponds to SR in two passes of the amplified PR pulse and arises from FBG filtering. A wider SR spectrum arises from the backward pass of the probe pulse through the amplifier. Obviously, at a constant amplifier pump power and a high duty cycle of the probe radiation, SR is generated mainly between optical pulses. Analysis of the optical spectra revealed that in the existing amplifier, the SR fraction could reach 50% of the total output power.

Bandpass filters are commonly used for spectral filtering of PR (see, e.g., [9]). In this case, a narrow-band filter with a centre transmission wavelength matched to that of the master laser is required. However, temperature drifts of the filter and laser source wavelengths can lead to their mismatch and, as a consequence, to a decrease in the filtering efficiency. In this work, a Gooch & Housego amplitude acousto-optic modulator (AOM) was used for spectral filtering of the probe radiation. The idea behind this approach is based on the fact that SR is generated predominantly between pulses. For this reason, if the amplified radiation is transmitted only at the time of generating each pulse, spectral filtering of the radiation is also possible. Moreover, by inverting the AOM transmission signal, the opposite effect can be achieved, when the total generated signal is filtered from the useful radiation with a wavelength near 1550 nm (a qualitative explanation is presented in Fig. 2b).

Three types of modulation were investigated in the experiments: the selection of only laser pulses at a wavelength of 1550 nm [laser radiation (LR) regime], the selection of only spontaneous radiation (SR regime), and also the absence of modulation, when both laser and spontaneous radiation completely passes through (LSR regime). Figure 2a shows the optical spectra corresponding to these regimes; it can be seen that the original amplified signal is well separated into LR and SR signals, when changing the type of modulation.

First of all, we compared the reflectograms obtained in different modulation regimes (Fig. 3a). Attention should be paid to the difference in signal levels at the beginning of the

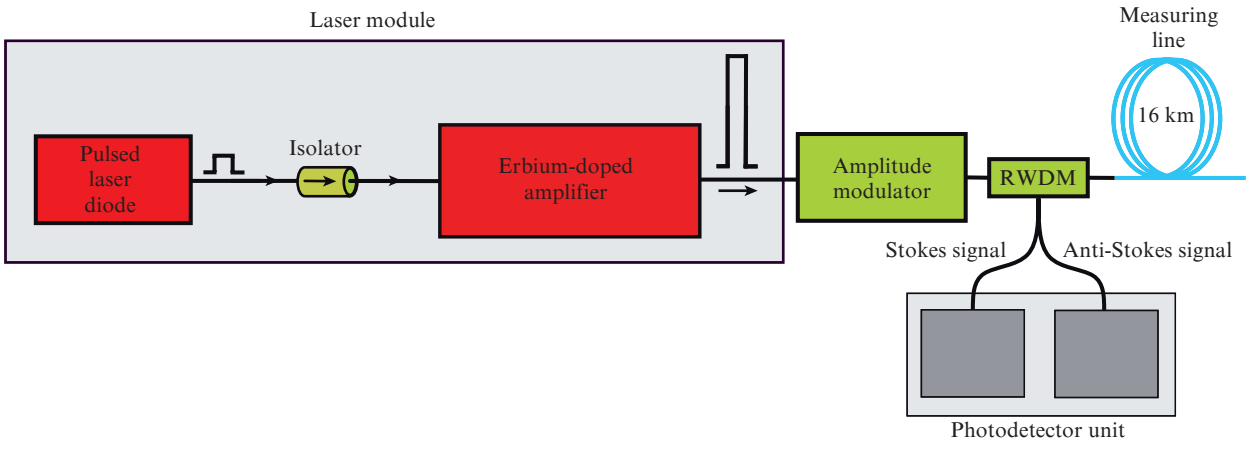

Figure 1. DFSS thermometry scheme with spectral filtering of radiation.

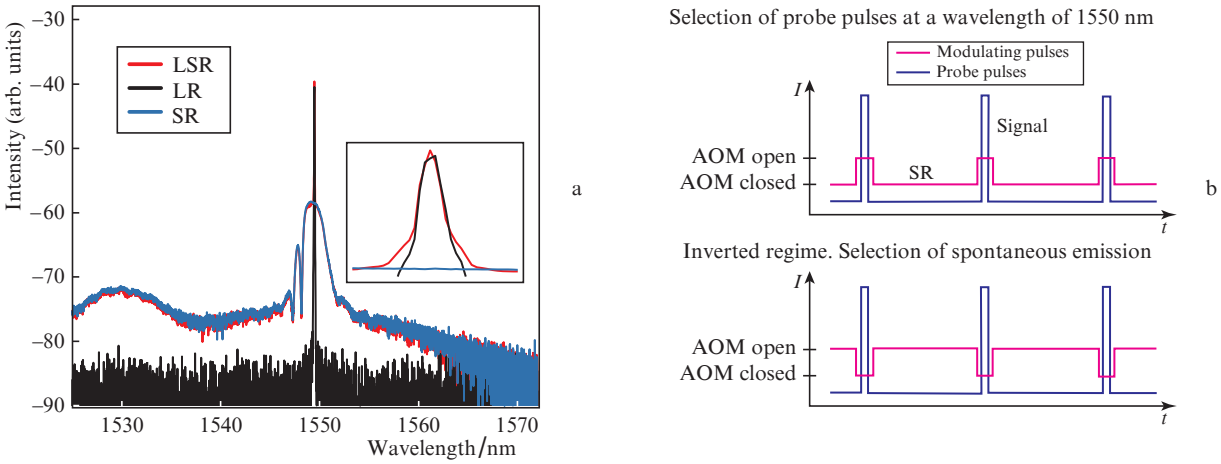

Figure 2. (Colour online) (a) PR spectra at the AOM output in different modulation regimes (the inset shows an enlarged image of the signal spectra) and (b) qualitative explanation of the spectral separation using an amplitude modulator.

line before the appearance of the probe pulse scattering signal (Fig. 3b). For the reflectogram in the LR regime, this level is seen to coincide with the zero value of the photodetector current (that is, with the level in the absence of a probe signal). The level at the beginning of the line for reflectograms in the LSR regime practically coincides with the level in SR regime, which allows concluding that the signal from SR raises the reflectogram as a whole. If this signal remains unchanged throughout the reflectogram measurement, this offset can be easily eliminated by using a low-pass filter or other similar methods. In further analysis of the reflectograms, it was assumed that the constant signal level at the beginning of the line is zero.

The resulting reflectograms were approximated by an exponential function of the form $R_{app}(z) = Ae^{-\alpha z} + D$, where D is the zero signal level at the beginning of the line (dashed curves in Fig. 3a). At first glance, the exponential dependence predicted by the theory of optical reflectometry describes well the reflectograms for the SR and LSR regimes. However, a careful examination of the curves corresponding to the experimentally measured reflectogram $R_{exp}(z)$ and its exponential approximation $R_{app}(z)$ showed their difference. Comparison of the residual differences $\Delta R(z) = R_{exp}(z) - R_{app}(z)$ for the reflectograms obtained in different modulation regimes is shown in Fig. 4. It is seen that with SR filtering, a noticeable 'flattening' of the residual difference to zero is observed, starting from a length of 2 km and up to the end of the measuring line. It should be also noted that the indicated effect of SR on the shape of the reflectograms is especially characteristic of the anti-Stokes component of scattering. Thus, we can conclude that when filtering spontaneous emission using AOM, the reflectogram is better described by an exponential function than without filtering.

Then, a similar analysis of the quality of the approximation was performed at different levels of amplification of the pump radiation in the amplifying channel. Figure 5a shows the quality parameter of the approximation of each reflectogram, calculated as a root-mean-square value of the residual difference $\left(\overline{\Delta R^2(z)}\right)^{1/2}$ depending on the value of the coefficient A of the exponential approximation. It is seen that filtering leads to a decrease in the rms value of the residual difference for both the Stokes and anti-Stokes spectral components. We also analysed the behaviour of the loss parameter obtained in the course of the approximation – the exponent α (Fig. 5b). It should be noted that the approximation parameters are practically independent of the reflectogram amplitude for both Stokes and anti-Stokes components with filtering. Only at high powers for LR modulation, the attenuation coeffi-

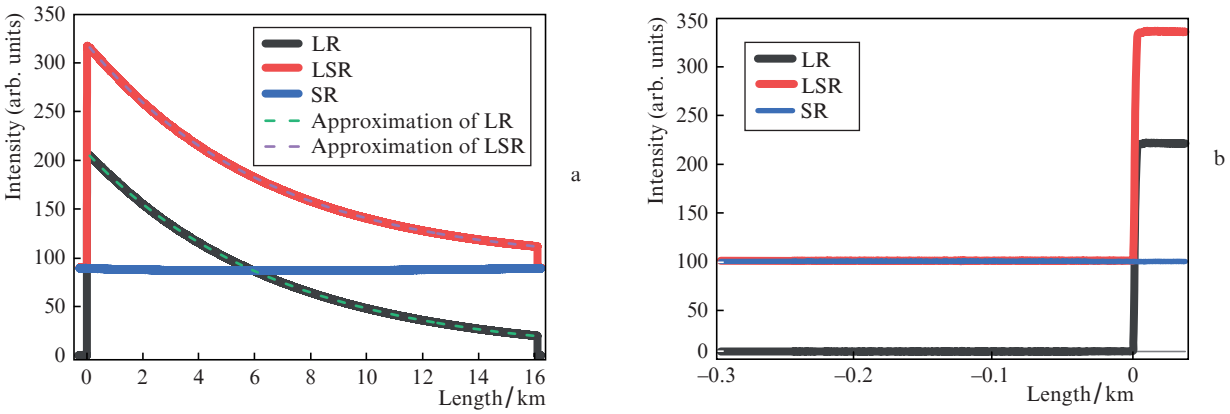

Figure 3. (Colour online) Reflectograms in different modulation regimes and their corresponding exponential approximations for the anti-Stokes signal (a) for the entire line and (b) on an enlarged scale.

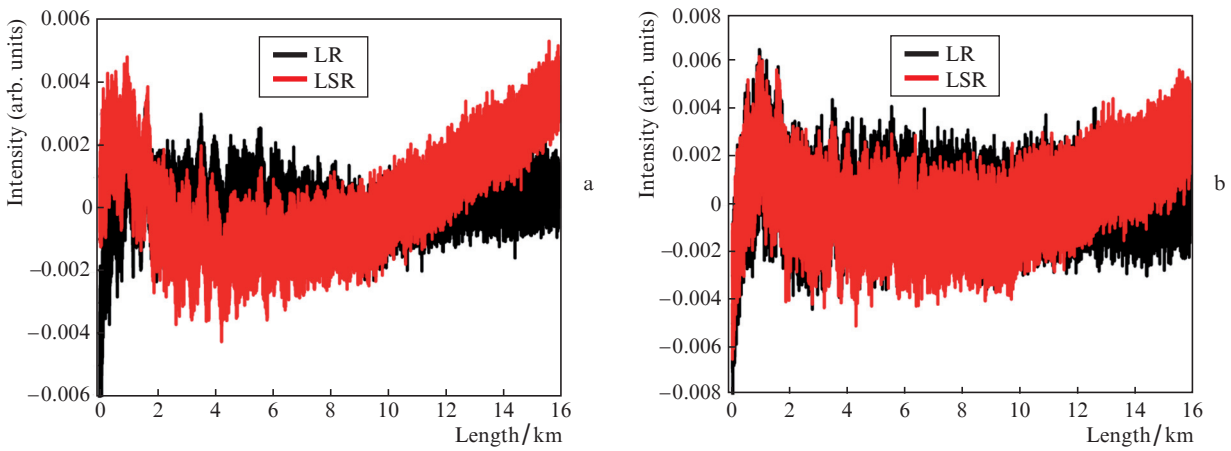

Figure 4. (Colour online) Residual differences $\Delta R(z)$ upon the exponential approximation of experimental reflectograms in LSR and LR regimes for (a) anti-Stokes and (b) Stokes components.

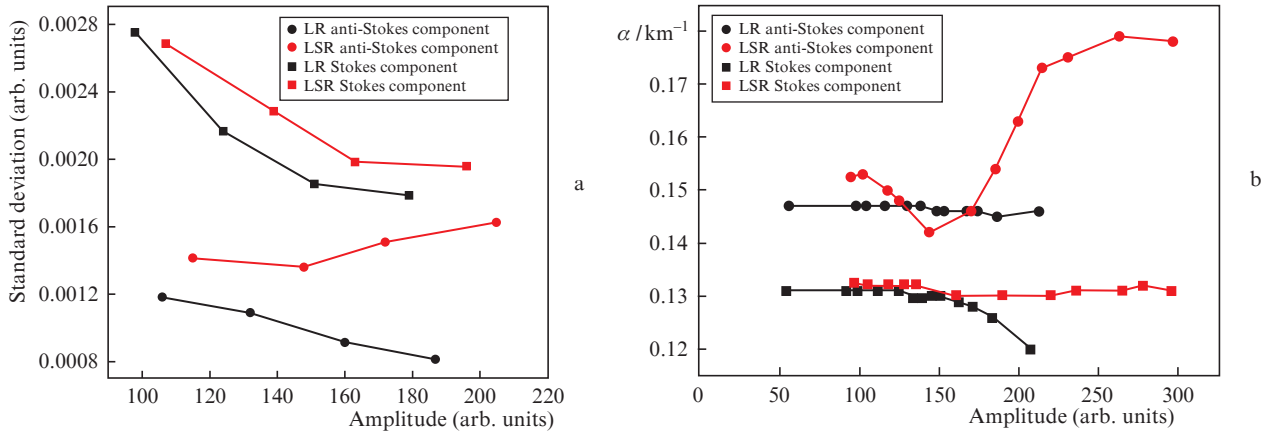

Figure 5. (Colour online) Comparison of the approximation quality parameter of the reflectograms (a) and the loss parameter α (b) depending on the amplitude of the reflectograms A in the LSR and LR modulation regimes for Stokes and anti-Stokes signals.

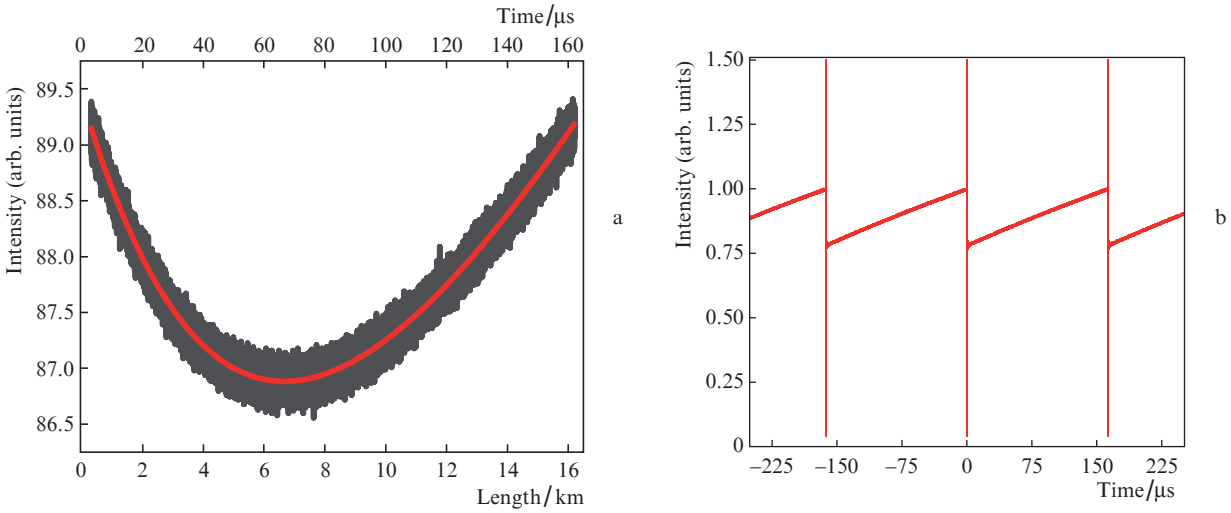

Figure 6. (Colour online) (a) Reflectogram of the anti-Stokes signal from SR with an approximating curve corresponding to formula (1) and (b) dynamics of the SR intensity.

cient of the Stokes component begins to decrease. The latter may be associated with the appearance of the Stokes component enhancement upon transition to the stimulated Raman scattering (SRS) regime. Note that in a similar situation for

LSR modulation, no noticeable change in α is observed, which can be explained by the combined effect of SRS and spontaneous noise.

A separate analysis of the reflectograms for the SR scattering signal (Fig. 6a) showed that there is a small variable component in the signal, which can affect the quality of the exponential approximation in the LSR regime. It can be seen from Fig. 6a that for SR the scattering response has the form of a parabola. Note that the value of the variable part of the reflectogram in the SR regime can reach 1% of the reflectogram amplitude in the LR regime. The intensity of the obtained reflectogram is well approximated by the expression predicted by the theory (see below):

$$I_{SE}(\tau) = Ae^{-k\tau} + B\tau + C, \quad (1)$$

where τ is the delay time between the beginning of the probe signal and the moment of arrival of the scattered signal. As will be shown below, this behaviour can be associated with the variability of the SR power itself. Indeed, the temporal dynamics of the spontaneous emission intensity, measured with a photodetector and an oscilloscope, demonstrates a sawtooth dependence (Fig. 6b) with a modulation amplitude of $\sim 20\%$ of the average value.

To determine the mechanism of the formation of the reflectogram signal from SR, the scattered radiation spectra were measured for the Stokes component in various modulation regimes (Fig. 7). It was found that the shape of the recorded spectrum arriving at the photodetector does not depend on the type of modulation (LR, SR, or LSR). Hence, we can conclude that the RS signal is formed even when the line is probed by spontaneous emission. A similar result was obtained for the anti-Stokes component. Thus, the RS signal from SR leads to deformation of the measured reflectograms. It should be noted that the signal at the Rayleigh wavelength in the Stokes and anti-Stokes channels is not observed due to the high level of the RWDM filtering used.

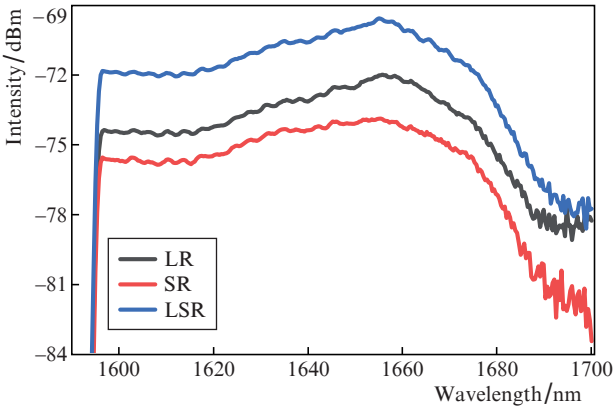

Figure 7. (Colour online) Scattered signal spectra for the Stokes component.

3. Discussion of the results

The performed experiments have shown that the presence of spontaneous emission leads to an additional nonexponential dependence of the reflectogram. The deviation reaches 1% of the reflectogram amplitude (see Figs 3 and 6a) in the middle of the measuring line length. Let us estimate the influence of this deviation on the accuracy of determining the temperature by the sensor. It is known that temperature data are determined by the intensity of the anti-Stokes signal I_{as} [1]. To eliminate the influence of the amplitude change because of linear losses, the temperature signal is normalised using Stokes as well as Rayleigh scattering signals. For simplicity, consider the case when we know the value of the linear loss α for signal normalisation. In this case, the temperature distribution is calculated by the expression [1]

$$T_{tem}(z) = S\left\{\ln\left[1 + q\frac{\exp(-\alpha z)}{I_{as}(z)}\right]\right\}^{-1}, \quad (2)$$

where S is the temperature sensitivity of the system, determined by the properties of the measuring fibre [1]; and q is a constant coefficient determined by the parameters of the measuring system, which is calculated from calibration measurements. Assume that the measuring fibre line is thermally stabilised at a constant temperature $T_{tem}(z) = T_0$. It can be expected that for such a line the change in the signal is caused only by linear losses, i.e., the scattering signal for the anti-Stokes component is described by the exponential function $I_{as}(z) = I_{as}(0)\exp(-\alpha z)$. In particular, this makes it possible to determine the constant coefficient q. However, as shown above, the intensity of this signal has the form $\tilde{I}_{as}(z) = I_{as}(0)\exp(-\alpha z) + Bz$. Substituting this dependence into expression (2), one can make sure that the calculated temperature distribution is not constant along the line. The estimates from the above expressions and the data obtained in the experiment show that the temperature measurement error could reach five degrees and increase with the line length due to an increase in the deviation of the signal intensity from the exponential dependence. Note that the actual error may be less than the estimated five degrees, since in practice a more complex normalisation of the scattering signals is used to calculate the temperature. However, even the use of these normalisations does not allow complete elimination of the above nonexponential addition of the line length to the measured signals due to the difference in losses at different wavelengths.

4. Calculation of the reflectogram shape

Let us find the shape of the reflectogram for a quasi-continuous optical signal. For simplicity, we assume that the time dependence of the intensity of quasi-continuous radiation can be described by a sawtooth function with a slope coefficient a and a repetition period T, shown in Fig. 8a. In other words, we assume that the change in the SR intensity at the period with the number n has the form $I(t) = at + b - (n-1)aT$, where b is the intensity at the beginning of each saw tooth. Based on the experimental results (Fig. 6b), such an approximation seems to be justified. It is known that the response for pulsed radiation scattered from a homogeneous fibre line has an exponential character, e^{-kt}, where k is the attenuation coefficient. Note that the final scattering signal is contributed by the signal generated not earlier than the time $\tilde{T}$ of the fibre line round-trip. For one period, this response at time τ can be expressed as a convolution function of two signals:

$$\int_{\tau-\tilde{T}}^{\tau} I(t)\exp[-k(\tau - t)]\,dt. \quad (3)$$

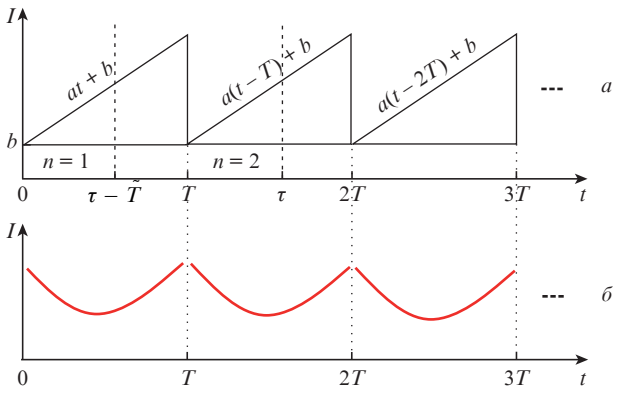

Figure 8. (Colour online) (a) Model time dependence of the intensity of the quasi-continuous signal SR and (b) the corresponding shape of the reflectogram.

Integration gives the final expression for the scattered signal from SR:

$$I_{SE}(\tau) = \frac{aT}{k} e^{kT} e^{-k\tau} + \frac{a}{k}\tau + \frac{b - aT}{k}. \quad (4)$$

Proceeding to the effective coefficients

$$A = \frac{aT}{k} e^{kT},\ B = \frac{a}{k},\ C = \frac{b - aT}{k},$$

we arrive at Eqn (1). When deriving expression (4), it was assumed that the pulse repetition period is close to the line round-trip time, $\tilde{T} \approx T$, and that the line is rather long, $e^{-kT} \ll 1$. It is worth noting that although dependence (4) was obtained for the interval $T < \tau < 2T$, its functional form (1) will be preserved for $0 < \tau < T$. From the time dependence (1), the coordinate dependence is easily obtained by the transformation $\tau = 2n_{eff}z/c$. Based on this, the parameters k and α are related as $\alpha = 2n_{eff}k/c$ (n_{eff} is the effective refractive index of the fibre). Analysis of expression (4) shows that when the intensity of spontaneous emission does not change with time (that is, $a = 0$), then the scattering signal from SR is also constant in time.

5. Conclusions

Thus, it is shown that the presence of an amplifier based on an erbium-doped fibre leads to the appearance of a time-dependent noise component in the probe signal. The sawtooth behaviour of the intensity of this radiation is due to the pulsed nature of the input signal: the intensity is minimal after the pulse, and then increases linearly with time. Despite the smallness of the peak amplitude of spontaneous emission relative to the peak amplitude of the pulse signal, it permanently has a nonzero value. As a result, the SR average power fraction can be as high as half the total PR power level, and the spontaneous emission is subject to RS, too. All this gives rise to a time-dependent scattering signal from SR. The obtained analytical expression for the SR signal reflectogram shape describes well the experimentally obtained dependences. The observed variability of the scattering signal leads, firstly, to a rise in the reflectogram, and secondly, to its deformation. Filtering the signal from SR using the AOM improves the reflectogram description with an exponential function. However, it should be noted that there is a deviation from it at the beginning of the reflectogram line (see Fig. 4), caused by other effects, the nature of which has not yet been established by us. The constancy of the reflectogram approximation parameters for the filtered signal is also shown, which is quite expected.

It is important to note that the observed effects are characteristic of short PR pulses with a low repetition rate. Thus, the described behaviour of the reflectograms is essential for sufficiently long DFSS's, the operation of which requires the use of pulses with a low repetition rate. In this case, an effective increase in spontaneous emission occurs between pulses. Estimates show that the described deformation of the trace can lead to a temperature measurement error of several degrees. It is expected that the proposed method for suppressing the influence of spontaneous emission using AOM will improve the metrological characteristics of DFSS's based on the analysis of the scattering signal amplitudes.

Acknowledgements. The work was performed within the framework of the State Assignment of the Institute of Automation and Electrometry, Siberian Branch of the Russian Academy of Sciences (IAE SB RAS) (No. AAAA-A19-119112990054-4) using the equipment of the Multiple-Access Center 'High-Resolution Spectroscopy of Gases and Condensed Matters' of the IAE SB RAS, Novosibirsk. The authors are grateful to A.G. Kuznetsov for providing the acousto-optic modulator.

References

1. Hartog A. *An Introduction to Distributed Optical Fibre Sensors* (Boca Raton: CRC Press, 2017).
2. Barrias A. et. al. *Sensors.*, **16** (5), 748 (2016).
3. Healey P. *J. Phys. E. Sci. Instrum.*, **19** (5), 334 (2000).
4. Dakin J.P. et. al. *Electron. Lett.*, **21**, 569 (1985).
5. Kuznetsov A.G., Babin S.A., Shelemba I.S. *Quantum Electron.*, **39** (11), 1078 (2009) [*Kvantovaya Elektron.*, **39** (11), 1078 (2009)].
6. Liu Z. et. al. *J. Fire Protect. Eng.*, **13** (2), 129 (2003).
7. Gorshkov B.G., Gorshkov G.B., Zhukov K.M. *Quantum Electron.*, **50** (5) 506 (2020) [*Kvantovaya Elektron.*, **50** (5), 506 (2020)].
8. Tanner M.G. et. al. *Appl. Phys. Lett.*, **99** (20), 201110 (2011).
9. Liu Y. et. al. *Opt. Express*, **26** (16), 20562 (2018).
10. Kuznetsov A.G., Kharenko D.S., Babin S.A., Tsydenzhapov I.B., Shelemba I.S. *Quantum Electron.*, **47** (10), 967 (2017) [*Kvantovaya Elektron.*, **47** (10), 967 (2017)].
11. Feng C., Kadum J.E., Schneider T., in *Fiber Optic Sensing – Principle, Measurement and Applications* (IntechOpen, 2019) pp 59–79.
12. Taranov M.A., Gorshkov B.G., Alekseev A.E., Potapov V.T. *Appl. Opt.*, **60**, 3049 (2021).
13. Parker T., Shatalin S., Farhadiroushan M. *First Break*, **32**, 61 (2014).
14. Shatalin S.V., Treschikov V.N., Rogers A.J. *Appl. Opt.*, **37**, 5600 (1998).
15. Rosolem J.B. et. al. *IEEE Photonics Technol. Lett.*, **17** (7), 1399 (2005).
16. Harun S.W. et. al. *IEICE Electron. Express*, **2** (6), 182 (2005).